Published in final edited form as:
Neuropsychologia. 2015 January ; 66: 246–258. doi:10.1016/j.neuropsychologia.2014.11.020.

Age Related Differences in Reaction Time Components and Diffusion Properties of Normal-Appearing White Matter in Healthy Adults

Yiqin Yang[1,2], **Andrew R. Bender**[1,2], and **Naftali Raz**[1,2,3]

[1]Institute of Gerontology, Wayne State University

[2]Department of Psychology, Wayne State University

Abstract

Deterioration of the white matter (WM) is viewed as the neural substrate of age differences in speed of information processing (reaction time, RT). However, the relationship between WM and RT components is rarely examined in healthy aging. We assessed the relationship between RT components derived from the Ratcliff diffusion model and micro-structural properties of normal-appearing WM (NAWM) in 90 healthy adults (age 18 to 82 years). We replicated all major extant findings pertaining to age differences in RT components and WM: lower drift rate, greater response conservativeness, longer non-decision time, lower fractional anisotropy (FA),greater mean (MD), axial (AD) and radial (RD) diffusivity were associated with advanced age. Age differences in anterior regions of the cerebral WM exceeded those in posterior regions. However, the only relationship between RT components and WM was the positive association between DR in the body of the corpus callosum and non-decision time. Thus, in healthy adults, age differences in NAWM diffusion properties are not a major contributor to age differences in RT. Longitudinal studies with more precise and specific estimates of regional myelin content and evaluation of the contribution of age-related vascular risk factors are necessary to understand cerebral substrates of age-related cognitive slowing.

Keywords

aging; brain; DTI; Ratcliff diffusion model; MRI

1. Introduction

Advanced age is reliably associated with reduced speed of processing (Cerella, 1985; Salthouse, 1991), but the neural underpinnings of that association remain unclear. Drawing on the findings that link response slowing to diffuse axonal injury (e.g., Felmingham,

[3]Correspondence address: 87 East Ferry St. Detroit, MI 48202, nraz@wayne.edu, telephone: +1-313-664-2617 .

Baguley, & Green, 2004), many studies attempted to demonstrate the association between age-related differences in integrity of the cerebral white matter and age-related slowing (see Gunning-Dixon & Raz, 2000; Madden, Bennett, & Song, 2009a for reviews). To date, the overwhelming majority of studies that examined relationships between speed of processing and diffusion properties of white matter have used mean or median reaction time (RT) on a variety of cognitive and perceptual tasks as the main indicator of speed of processing. However, most do not take into account heterogeneity of RT that usually shows markedly non-Gaussian distribution, and has been long conceptualized as complex phenomena comprised of multiple components (Salthouse, 1981) In addition, procedures based on indices of central tendency, such as Donders' subtractive method (Donders, 1969) and Sternberg's additive-factor method (Sternberg, 1969) do not take into account RT distribution and assume no temporal overlap between stages - an assumption that is virtually impossible to sustain.

Many approaches have been proposed to address the heterogeneous nature of RT and quantify its components. Although ex-Gaussian function fits RT data well, its parameters do not reflect clearly interpretable mental process (Matzke & Wagenmakers, 2009). Notably, all traditional methods do not take into account speed-accuracy trade-offs, which is especially important in study of age-related differences because older adults tend to emphasize accuracy more than younger adults do (Salthouse, 1979). The mathematical model proposed by Ratcliff (1978) was designed to overcome these limitations. Ratcliff's diffusion model successfully accounts for all aspects of RT data and decomposes them into meaningful mental processes: rate of information acquisition, response conservativeness and time spent on non-decision processes (Ratcliff & McKoon, 2008).

At the time of this writing, there is only one study of the associations between white matter properties and two of three RT components derived from the diffusion model: drift rate and non-decision time (Madden, Spaniol, et al., 2009b). That study has several limitations. First, the diffusion parameters were estimated with a simplified version of the diffusion model (EZ), which was designed only for exploratory purposes and did not provide precise parameter estimates (Ratcliff, 2008a). Second, only two relatively small extreme-age groups were compared, and age-related differences were not investigated across the adult life span. Third, that study evaluated only two RT components, drift rate and non-decision time, while the neuroanatomical substrates of response conservativeness remained unexamined. Finally, in assessing the associations of RT components with the white matter indices, the study did not separate white matter hyperintensities (WMH) from the normally appearing white matter and thus confounded the influence of these breaches on the diffusion parameters of white matter. Because WMH burden increases with age, is associated with age-related slowing (Gunning-Dixon & Raz, 2000), has substantially altered diffusion properties (Maillard et al., 2013) and may account for a significant share of age-related differences in diffusion indices (Davis, Kragel, Madden, & Cabeza, 2012, Vernooij et al., 2008), controlling for the effects of WMH is essential for understanding the relationship between diffusion parameters of white matter and speed of processing.

To address these limitations, we investigated the relationship between age related differences in diffusion properties of the cerebral white matter and three RT components

derived from the Ratcliff diffusion model: the rate of information accumulation (drift rate), response conservativeness (boundary separation), and non-decision time by taking the following approach. First, we applied the full diffusion model to decompose RT into three components as specified in the full Ratcliff model. Second, we studied healthy adults spanning a wide age range. Third, we used the indices of white matter diffusion derived from diffusion tensor imaging (DTI) data restricted to normal appearing white matter after removing the WMH. Fourth, we used tract-based spatial statistics (TBSS, Smith et al., 2006), to identify multiple white matter pathways: the superior longitudinal fasciculus, the uncinate fasciculus, the cingulum adjacent to cingulate gyrus portion, the genu, body, and splenium of the corpus callosum, and the anterior, and posterior limb of the internal capsule. Our selection of pathways was based on the extant literature. White matter integrity in anterior and superior regions contributed to perceptual speed (Bucur et al., 2008; Kennedy & Raz, 2009; Turken et al., 2008). DTI parameters of uncinate fasciculus were associated with performance on tasks assessing executive functioning in older adults (Davis et al., 2009), suggesting this tract might be involved in response conservativeness. Frontal-striatum network was implicated in cognitive control (Liston et al., 2006), and the latter had been shown to play a role in response conservativeness (Dutilh et al., 2012; Saunders & Jentzsch, 2012). DTI parameters in the cingulum were associated with information processing speed (Sasson, Doniger, Pasternak, Tarrasch, & Assaf, 2012). FA in the posterior region was associated with sensory-motor responses (Sullivan et al., 2001). We also took care in selecting the skeleton locations that would be the least sensitive to multiple threats to validity of the TBSS analytic approach used in this study. Specifically, we avoided potentially relevant regions, such as fornix, because of its particular sensitivity to misregistration and noise (Smith et al., 2006; Bach et al, 2014). We modeled the relationships between RT parameters and white matter diffusion features in a structural equations modelling (SEM) path analysis framework, a multivariate approach that takes into consideration the mutual influence among the predictors and assessing the unique contribution of predictors to criteria. The extant studies indicate that anterior white matter regions and tracts evidence greater age-elated differences in comparison to posterior regions (the anterior-posterior gradient of aging hypothesis) (Head et al., 2004; Madden et al., 2009a, and the connections between high-order association cortices are more relevant to speed of information processing than to motor speed (Kennedy & Raz, 2009; Kerchner et al., 2012; Madden et al., 2009a). We therefore expected that age-related differences in two decision components of RT (drift rate and response conservativeness) would correlate with diffusion properties of anterior rather than posterior white matter, and would be related to the indices of white matter organization in the association and commissural rather than projection fibers. In contrast, we hypothesized age-related differences in non-decision time to show stronger associations with white matter diffusion properties in posterior rather than anterior regions, and in projection rather than association or commissural fibers.

2. Method

2.1. Participants

Participants were healthy community volunteers from the Metro Detroit area who were enrolled in a longitudinal study of healthy aging. They were recruited through

advertisements in the local media and screened via a telephone interview and an extensive health questionnaire. Participants were ineligible if they reported history of cardiovascular disease, neurological or psychiatric conditions, head trauma with loss of consciousness for more than 5 min, treatment for drug and alcohol problems, or a habit of taking more than three alcoholic drinks per day. Persons with diagnosis of diabetes or thyroid dysfunction were also excluded from the study, as were those taking any anxiolytics, antidepressants or anti-seizure medication. None of the participants resided in a nursing home or an assisted-living facility.

All participants had corrected visual acuity of 20/50 or better (Optec 2000 apparatus; Stereo Optical, Chicago, IL) (ICO, 1984) without color blindness, and hearing of 40 dB or better for frequencies of 500–4,000 Hz (MA27 audiometer; Maico, Eden Prairie, MN) (WHO, 1991); all were native English speakers, with a minimum of a high school education (or a GED diploma), and were consistently right-handed as determined by Edinburgh Handedness Questionnaire (Oldfield, 1971) score of 75% and above. To screen for dementia and depression, we used the Mini-Mental State Examination (MMSE: Folstein, Folstein, & McHugh, 1975), with a cut-off of 26 (O'Connor et al., 1989) and depression questionnaire (CES-D; Radloff, 1977), with a cut-off of 15 (Burns, Lawlor, & Craig, 2002). The participants provided written informed consent in accord with the guidelines of Wayne State University Institutional Review Board. In addition, for this study, the participants were screened for history of hypertension and were excluded if they were taking anti-hypertension medication. Participants who had no MRI data due to either being claustrophobic or having metallic implants were not included in this study.

Although the initial sample consisted of 100 participants, four participants had low rate of usable RT data identified by exponentially weighted moving average (EWMA) method (less than 90%) and the RT data of six participants did not fit the RT model. Thus, the total sample with complete data consisted of 90 healthy normotensive adults (90% of the original sample), 18 to 82 years of age. The excluded participants did not differ from the remaining sample on age ($t = -1.30$, $p = .22$), education ($t = -.54$, $p = .60$), sex ratio ($\chi^2 = -.05$, $p = .83$), and ethnic origin ($\chi^2 = -.15$, $p = .70$) and thus were considered missing at random. Sample demographic information is presented in Table 1.

2.2. Reaction Time Task and Analysis

2.2.1. Reaction time task—RT data were collected from a two-choice letter discrimination task (Thapar, Ratcliff, & McKoon, 2003). Participants were seated in front of a 19-inch liquid crystal display (LCD) computer monitor in a quiet room. They were asked to sit comfortably and lean back in the chair. The height of the monitor was adjusted so that the midpoint of the monitor was at the subject's eye level. The distance from the middle of the screen to the outer corner of participants' eye was 60 cm. Participants were required to maintain their positions after the distance had been established. The responses were entered via a custom-built seven-button response box. The experimenter was present in the room throughout the testing to ensure compliance with the instructions and note participant behaviors that might have affected data validity.

The letter discrimination task was administered in two sessions, of about 36 minutes each. The sessions consisted of six blocks (108 trials per block) that were preceded by two practice blocks and lasted approximately 4 minutes each. The participants were required to take brief breaks between blocks. The total number of trials for two sessions was 1296; 216 trials per stimulus duration. The same stimuli, letter pairs P/R, O/Q, I/J, F/E, C/G, and V/W, were used on all trials.

In the task, two letters were displayed, one on the left and the other on the right edge of the screen. The letters remained on the screen for the duration of the block. In the middle of the screen, a white cross (font: courier new bold, size: 40) appeared for 500 ms, after which the target letter was displayed for one of the six durations (13, 26, 39, 52, 66, and 80 ms), followed by a mask. The task of participants was to identify the target letter and decide whether it was the same as the letter on the left or the letter on the right edge of the screen. Participants received a feedback from the screen when they responded too quickly or too slowly. Because the order of the letter pairs differed between two sessions, the order of the sessions was counterbalanced across participants.

2.2.2. RT - Diffusion model analysis—The two-choice RT data were analyzed with Diffusion Model Analysis Toolbox (DMAT, Vandekerckhove & Tuerlinckx, 2008), which estimates parameters by minimizing a negative multinomial loglikelihood function. Before fitting the diffusion model, RT data extreme values were excluded using the lower cutoff of 200 ms and the upper cutoff of 1799 ms. In addition, a combination of EWMA and mixture model methods was applied to deal with the remaining outliers. Starting point was fixed in the middle between the two response boundaries. To assess whether the parameters of the diffusion model reflects relevant experimental manipulation (i.e., variation of stimulus duration), two different models were fitted to each participant's data. The models differed in one parameter setting: v, the drift rate. Because v reflects the quality of information obtained from the stimulus, and was expected to be affected by the experimental manipulation (variation of stimulus duration) (Thapar et al., 2003; Voss et al., 2004), it was allowed to vary in one model. In another model, v was restricted and drift rates for all conditions were set to be equal. All other parameters were set to be invariant across experimental conditions in both models. The goodness-of-fit indices for two models were computed for each participant and for all of them, the v free model gave the significant better fit to the data (p = 0). The preference of the v free model over the v restricted model was also suggested by reduction in AIC and BIC values for the v free model, except in one case, in which one index, BIC, showed a minute increase of .002%. This suggested that the diffusion model was sensitive to the experimental manipulation of RT data. Because an exceedingly high accuracy rate in easier conditions with longer durations of presentation affected the fit of the diffusion model, only the data from the first three (more difficult) conditions were considered for drift rate analyses.

2.3. MRI Data Acquisition and Processing

2.3.1. MRI protocol—Imaging was performed on a 3T MRI system (Siemens MAGNETOM Verio™, Erlangen, Germany) with a 12-channel radio frequency (RF) coil. The acquisition session included several sequences, of which only the diffusion tensor

imaging (DTI) sequence was used for this study. The DTI data were acquired in the axial plane with a single shot echo-planar imaging sequence, with the following parameters: repetition time (TR) 12000 ms, echo time (TE) 124 ms, 20 diffusion directions, 2 averages, 50 contiguous slices, field of view (FOV) = 256×256 mm^2, voxel size = 1.3×1.3×2 mm^3, b = 1000 s/mm^2, GRAPPA acceleration factor 2. The sequence also included two images without a diffusion gradient (b = 0). Acquisition duration was 9:02 min. In addition, T2- and T1-weighted sequences were acquired and all MR scans were examined for signs of space-occupying lesions and all participants were free of pathological findings.

2.3.2..Image processing—Diffusion weighted images were analyzed using FMRIB's Diffusion Toolbox (FDT) from the FMRIB Software Library (FSL; http://fsl.fmrib.ox.ac.uk/fsl/fslwiki/). Motion artifacts and eddy current distortions were corrected by Eddy Current Correction tool in FDT, which aligns each diffusion-weighted image to the b0 image. The gradient orientations were rotated accordingly as well. The eddy current-corrected 4D volumes were then divided into separate acquisitions which were subsequently averaged to produce a single 4D volume containing one b = 0 image and 20 gradient directions. After this step we proceeded to control the influence of WMH and CSF spaces using a method that combines previously published approaches (Davis et al., 2012; Sasson, Doniger, Pasternak, & Assaf, 2010). The first averaged image that did not have gradient applied (i.e., b = 0) was used to generate a binary brain mask with the Brain Extraction Tool (BET; Smith, 2002). A WMH-free brain mask was created with the following steps. First, FMRIB's automated segmentation tool (FAST; Zhang, Brady, & Smith, 2001) was used to segment b0 image into four separate classes based on voxel intensity: CSF, WMH, gray and white matter. At the next step, fslmaths command was used to create a WMH-free brain mask by combining segmented gray and white matter images and binarizing the combined image. DTIFIT was used to fit a diffusion tensor model at each voxel included in the brain mask and WMH-free brain mask to generate the diffusion maps for whole and normal-appearing white matter (NAWM).

Skeletonized fractional anisotropy (FA) data were generated following the TBSS processing pipeline (after Smith et al. 2006). First, individual FA image was non-linearly aligned to the FMRIB58_FA template. Next, transformed FA images were averaged and thinned to create a skeletonized mean FA image. The mean FA skeleton was thresholded at 0.2 to exclude voxels containing gray matter or CSF. Finally, the aligned FA image of each participant was projected onto the skeleton by filling each skeleton voxel with FA values from the nearest relevant tract center, resulting in a skeletonized FA image. Skeletonized diffusivity maps for mean (MD), axial (AD) and radial (RD) diffusivity were generated using spatial transformation parameters obtained in the initial FA analysis. Following these steps, selected skeletonized maps of all four DTI indices in whole white matter and normal-appearing white matter were generated. All skeletonized maps were further thresholded such that voxels with FA less than .2 or larger than 1.0 were not included to reduce the noise of DTI data.

White matter tracts were labeled according to ICBM-DTI-81 white-matter labels atlas (Mori, Wakana, Nagae-Poetscher, & van Zijl, 2005), which was generated by mapping DTI data of 81 normal individuals to a template image. Because the skeletonized DTI maps and the atlas were both in the same standard space, no additional registration step was required.

Fslmaths was used to create masks for individual white matter tracts relevant in this study. DTI parameters of each white matter tract, with and without WMH, were extracted for all participants by applying fslstats procedure. Due to limited number of slices, there was incomplete coverage of the anterior temporal lobe for most participants. Therefore, DTI indices from the uncinate fasciculus were eliminated from all the analysis.

2.4. Data Conditioning

To minimize rounding errors and scaling artifacts, the diffusivity values were multiplied by a factor of 1000. Before statistical analyses, all RT and MRI data were checked for outliers and violations of normality. If deviations from normality or significant outliers were identified, the data were log-transformed. If the log-transformation failed to reduce the skew, the data were winsorized instead. Specifically, logarithmic transformation was performed on DA of the left posterior limb of the internal capsule in normal appearing white matter. Winsorization was carried out on FA of the left and right anterior limb of the internal capsule, right superior longitudinal fasciculus, and the splenium of the corpus callosum in normal appearing white matter; MD of the genu of the corpus callosum in both normal appearing and whole white matter, and the left and right anterior limb of the internal capsule in whole white matter; DA of the left and right superior longitudinal fasciculus in normal appearing white matter, the left superior longitudinal fasciculus and the left and right anterior limb of the internal capsule in whole white matter; and DR of the genu of the corpus callosum in normal appearing white matter, and the left and right anterior limb of the internal capsule in whole white matter. After the described data conditioning, all variables were either normally distributed or not significantly skewed. To avoid scaling discrepancy, all variables were standardized before SEM analyses. To reduce the number of variables in the path models, standardized drift rates from the three conditions were averaged to yield a single composite score (v). DTI indices of white matter tracts from both hemispheres were also averaged. Because the extant literature does not report lateral differences in associations between the RT and DTI parameters, we had no reason to hypothesize such relationships and opted for reducing the number of tested paths and reducing the risk for spurious findings by aggregating the measurements over the two hemispheres.

2.5. Statistical Analyses

2.5.1. General linear models—To investigate age-relate differences on RT components and DTI indices, we used separate general linear models (GLM). In these models, each RT component or DTI indices served as dependent variables, while age and sex were independent variables. The possible interactions between age and sex were also included in the model, and removed if the interaction terms turned to be nonsignificant ($p > .10$). For DTI indices analysis, white matter tracts served as the within-subject (repeated measure) factor.

2.5.2 Path analysis—We used SEM-based path analyses to assess whether age differences in RT components were associated with individual differences in white matter diffusion properties. SEM was performed using maximum likelihood estimation in Mplus 7 (Muthén & Muthén, 2012). Model fit is considered good if χ^2 is nonsignificant or $\chi^2/df < 2$,

both comparative fit index (CFI) and Tucker–Lewis Index (TLI) are more than .95, and root mean square error of approximation (RMSEA) is less than .06 (Hu & Bentler, 1999).

Separate models were fitted for each DTI index because each reflects different property of the white matter. Only the white matter tracts and RT components that showed significant association with age from previous analyses were included in the SEM step. Significance of the quadratic component of association with age was formally tested for DTI indices that displayed apparent nonlinearity on scatter plots. Each set of analyses started with a hypothesis-based target model. Then, constrained or unconstrained models were generated by eliminating statistically non-significant paths and adding paths based on modification indices generated from previous analyses and theoretical perspective. Finally, the goodness of fit among the hierarchically nested models was compared and a most parsimonious and best fit model was obtained.

Because age-related differences in diffusion properties of white matter might be influenced by individual differences in cognition (Chiang et al., 2011), we evaluated two alternative models: a reversed-path and a correlational. The model specification was the same as each final model except for reversing the path direction between measures of RT components and DTI indices of white matter tracts in the reverse model and replacement of directional paths with correlations in the correlation model.

3. Results

3.1. Age-related Differences in Drift Rate, Response Conservativeness, and Non-Decision Time

The descriptive statistics and zero-order correlations of age with accuracy and response time across six conditions are presented in Table 2. Older age was associated with decreased response accuracy and increased response time for all conditions. Table 3 contains the descriptive information of three RT components.

The GLM analyses revealed significant main effects of age on all three components of RT. Advanced age was associated with slower drift rate [F (1, 87) = 34.31, $p < .001$], greater response conservativeness [F (1, 87) = 5.32, $p < .05$], and slower non-decision time [F (1, 87) = 31.57, $p < .001$] (see Figure 1). Neither the main effect of sex nor age × sex interaction was significant.

3.2. Diffusion indices in the normal-appearing white matter: Age and sex differences

Zero-order correlations between age and DTI indices across white matter tracts are presented in Table 4. Scatter plots of age differences in DTI-derived indices of white matter diffusion properties in each examined region are presented in Figures 2-5 below.

3.2.1. Fractional anisotropy (FA)—The GLM analysis revealed no age differences across the white matter tracts: main effect of age F (1, 86) = 1.35, ns. However, there was a significant tract × age interaction, F (6, 516) = 14.12, $p < .001$, indicating that the magnitude of age differences varied across the tracts. Neither the main effect of sex nor age × sex interaction was significant. Decomposition of the interaction revealed a negative age-FA

association in the genu, the anterior limb of the internal capsule, and the cingulum; but neither the body, nor splenium of the corpus callosum, nor the superior longitudinal fasciculus. There was a positive age-FA association in the posterior limb of the internal capsule (see Table 5).

3.2.2. Mean diffusivity (MD)—There was a significant main effect of age, F (1, 86) = 11.37, $p < .01$; advanced age was associated with higher MD across the examined white matter tracts. However, a significant sex × age interaction, F (1, 86) = 4.58, $p < .05$, indicated that the overall effect of age on MD was significant in men: F (1, 28) = 10.07, $p < .01$, but not in women: F (1, 58) = 1.13, $p = .29$. A significant tract × age interaction, F (6, 516) = 3.08, $p < .01$, indicated that the magnitude of age differences varied across the white matter tracts. Decomposition of this interaction showed age-related increase in MD in the genu, and body of the corpus callosum; the posterior limb of the internal capsule; and the cingulum; but not in the splenium of the corpus callosum, the anterior limb of the internal capsule, or the superior longitudinal fasciculus (see Table 5). There was a significant tract × sex interaction, F (6, 516) = 3.12, $p < .01$, indicating that MD was higher for women than for men in the cingulum, F (1, 86) = 5.90, $p < .05$, and the internal capsule: anterior, F (1, 86) = 9.69, $p < .01$; posterior, F (1, 86) = 7.44, $p < .01$.

3.2.3. Axial diffusivity (DA)—The GLM analysis revealed a significant main effect of age, F (6, 516) = 5.52, $p < .01$: advanced age was associated with increased DA across white matter tracts. There was a significant main effect of sex, F (1, 86) = 3.99, $p < .05$, with higher DA in women compared to men. A significant tract × age interaction, F (6, 516) = 4.19, $p < .001$, indicated that the effect of age differed across white matter tracts. Simple effects decomposition of this interaction revealed a positive association with age in the genu, and body of the corpus callosum; the posterior limb of the internal capsule; but not the splenium of the corpus callosum; the anterior limb of the internal capsule, the superior longitudinal fasciculus; or the cingulum (see Table 5). A significant tract × sex interaction, F (6, 516) = 2.68, $p < .05$, was due to DA being higher in the internal capsule of women compared to men: in the anterior limb, F (1, 86) = 7.82, $p < .01$, and the posterior limb, F (1, 86) = 8.71, $p < .01$.

3.2.4. Radial diffusivity (DR)—We observed a significant main effect of age, F (1, 86) = 12.74, $p < .01$, showing that advanced age was associated with higher DR across the white matter tracts. A significant tract × age interaction, F (6, 516) = 2.88, $p < .01$, indicated differential associations with age across white matter tracts. Advanced age was associated with higher DR in the genu, body of the corpus callosum; the anterior limb of the internal capsule; the superior longitudinal fasciculus; and the cingulum; but not in the splenium of the corpus callosum, and the posterior limb of the internal capsule (see Table 5). There was a significant tract × sex interaction, F (6, 516) = 3.42, $p < .01$, as DR was higher in women than in men in the anterior, F (1, 86) = 8.67, $p < .01$, and the posterior limb of the internal capsule, F (1, 86) = 4.60, $p < .05$, and the cingulum, F (1, 86) = 5.88, $p < .05$. A sex × age interaction was marginally significant ($p = .052$), and simple effects analyses showed that the age differences in DR were significant only in men: F (1, 28) = 10.69, $p < .01$, but not in women: F (1, 58) = 1.85, $p = .18$.

3.3. Comparison of age-DTI correlations in normal-appearing and whole white matter

Correlations between age and DTI indices in normal-appearing and whole white matter were compared using Steiger's *Z* (Table 6). For FA, relatively stronger negative age association was observed in the body and splenium of the corpus callosum, the anterior limb of the internal capsule in whole than in normal appearing white matter. For DR, age correlation was stronger in the genu of the corpus callosum in whole than in normal appearing white matter. For FA, MD, DA, and DR, positive correlation with age was greater in the posterior limb of the internal capsule in normal appearing than in whole white matter. Overall, age-related differences in DTI indices from whole white matter are greater than in those that were estimated in normal-appearing white matter regions (see Table 6).

3.4. Age, DTI Indices and RT Components

Three subsets of the path models investigated the contribution of individual differences in FA, DA, and DR to age differences in RT components. Because MD is an index that includes both DA and DR, we did not include it in the models. To account for multiple comparisons (i.e. testing three models for FA, DA, and DR), the nominal $\alpha = .05$ was adjusted to Bonferroni $\alpha' = .0166$.

The final model for FA fitted the data well (see Table 7 for the goodness-of-fit indices). The analysis revealed no significant directional path between FA and any RT components. There was a negative association between FA in the cingulum and response conservativeness ($p = .01$), and a positive association between FA in the posterior limb of the internal capsule and non-decision time ($p = .036$). Advanced age was associated with decreased FA in the genu of the corpus callosum, the cingulum, and the anterior limb of the internal capsule, but increased FA in the posterior limb of the internal capsule. Older age was associated with lower drift rate, higher response conservativeness and longer non-decision time. See Figure 6 for the final model. However, the association between age and FAs in the anterior limb of the internal capsule ($p = .027$) and cingulum ($p = .019$), between FA in the posterior limb of the internal capsule and non-decision time became nonsignificant after Bonferroni correction, although the association between age and response conservativeness ($p = .016$) remained significant.

As shown in Table 7, the final model for DA fitted the data well. There were linear and quadratic associations between age and DA in the genu and the body of the corpus callosum and in the posterior limb of the internal capsule. The directional path from DA in the genu of the corpus callosum to drift rate bordered on significance ($p = .05$) (Figure 6). Both the reversed model and correlational model fitted the data equally well (see Table 7). The directional path from drift rate to DA in the genu of the corpus callosum and the correlation between these two variables were marginally significant ($p = .07$). Thus, none of these paths between DA in the genu of the corpus callosum and drift rate was significant after Bonferroni correction.

The final model for DR showed good fit according to multiple goodness-of-fit indices (see Table 7). Advanced age was lineally associated with increased DR in the genu of the corpus callosum. There were quadratic associations between age and DR in the body of the corpus

callosum, the anterior limb of the internal capsule, and the cingulum. There were positive directional paths from DR in the genu of the corpus callosum to drift rate ($p = .026$), and from DR in the body of the corpus callosum to non-decision time ($p = .031$). Because the model with reversing directional paths simultaneously did not converge, two reversed-direction models (the v reversed model and the ter reversed model) with changing one directional path each time were generated. They fitted the data well (see table 7). There were significant reversed directional paths between DR in the genu of the corpus callosum and drift rate ($p = .022$), and between DR in the body of the corpus callosum and non-decision time ($p < .01$). The well fitted correlational model (see table 7) revealed that the correlations between DR in the genu of the corpus callosum and drift rate ($p = .02$), and between DR in the body of the corpus callosum and non-decision time ($p < .01$) were significant (Figure 6). However, the association between DR in the genu of the corpus callosum and drift rate became nonsignificant after Bonferroni correction. After the correction, higher DR in the body of the corpus callosum was associated with longer non-decision time.

To examine whether the results were affected by exclusion of WMH, we repeated the analyses on the whole white matter. We found that smaller FA in the body of the corpus callosum was related to increased non-decision time ($p = .013$), whereas FA in the cingulum was negatively related to response conservativeness ($p = .032$). Greater DR in the genu of the corpus callosum was associated with higher drift rate ($p = .037$) and higher DR in the cingulum was related to increased response conservativeness ($p = .037$). Higher DR in the body of the corpus callosum was related to increased non-decision time ($p = .010$). There was no significant association between DA of any white matter tracts and RT components. However, the only significant association after Bonferroni corrections was that between smaller FA and higher DR in the body of the corpus callosum with prolonged non-decision time.

4. Discussion

4.1. Age-related Differences in RT components and DTI indices

The results revealed that advanced age was associated with lower drift rate, longer non-decision time and greater response conservativeness. These findings extend the observations reported by Ratcliff and colleagues in extreme age groups to an adult life-span sample (Ratcliff, 2008b; Ratcliff, Thapar, & McKoon, 2001, 2006, 2007; Thapar, Ratcliff, & McKoon, 2003).

As commonly reported in the literature (e.g., Sullivan, Rohlfing, & Pfefferbaum, 2010; Madden et al., 2009a), lower FA and greater MD, DA and DR were associated with advanced age in several examined white matter tracts in normal-appearing white matter. The observed anterior-posterior gradient of negative age differences in FA and positive age differences in diffusivity measures of several white matter regions were also consistent with previous findings (Head et al., 2004; Sullivan & Pfefferbaum, 2006; Sullivan et al., 2010). Although age-related increase in DR has been interpreted as a sign of myelin loss (Madden et al., 2009a), current evidence indicates that such differences are not specific to myelination unless the direction of the principle eigenvector is aligned with the corresponding tissue

architecture, which is not the case in areas with high density of crossing fibers or in voxels with partial volume (Wheeler-Kingshott & Cercignani, 2009).

We observed stronger associations between age and DTI indices in men than in women in several white matter tracts. This finding is in contradiction to an earlier report suggesting no sex difference in age-DTI associations (Inano, Takao, Hayashi, Abe, & Ohtomo, 2011). The reason for the discrepancy is unclear. Lack of screening for vascular diseases in that study may account for the discrepancy with our findings obtained in healthy adult. In an age-heterogeneous sample, vascular risk and sex may interact in modifying the association between age and DTI indices. Therefore, the effect of sex might be masked across people with different vascular risk factors. Indeed, Kennedy and Raz (2009) found a significant age × sex × hypertension interaction, with no significant age-MD association for hypertensive men, but highly significant association for normotensives, whereas the correlations between age and MD was somewhat higher in hypertensive women compared to their normotensive counterparts. This finding underscores the importance to take into consideration of vascular risk factor as a modifier of brain aging. In this study, we did not have a sufficient number of participants with hypertension to merit a separate analysis and therefore, restricted our sample to normotensive individuals.

Notably, all the reported age differences in DTI-derived indices were observed in the normal-appearing white matter. As the analyses of the whole white matter (with WMH included) revealed stronger associations with age, it is apparent that studies that fail to account for WMH contribution to DTI indices over-estimate age-related differences. Nonetheless, even after exclusion of the WMH, white matter of healthy older adults still presents evidence of reduced organization and degraded microstructure. Interestingly, in contrast to other examined regions, *positive* correlations with age were observed for DTI-derived indices in the posterior limb of the internal capsule, and these correlations were greater in the in normal appearing rather than in whole white matter. Although the underlying mechanism for this observation is unclear, iron accumulation in this area might play a role, as the presence of non-heme iron leads to increase anisotropy by introducing local field inhomogeneity (Pal, 2011). Moreover, increased iron content has been found in normal-appearing white matter and at the edges of WMH (Bagnato et al., 2011; Paling et al., 2012). In the future studies, this phenomenon may be assessed by combining iron imaging with assessment of WM organization and regional myelin content.

4.2. Association between age-related DTI Indices and RT Components

The results revealed no significant associations between normal WM FA or DA and any RT parameters. The only significant finding that survived Bonferroni correction was the associations between higher DR in the body of the corpus callosum and longer non-decision time. In the whole WM (including WMH), the same association was observed in addition to the association between lower FA and prolonged non-decision time. Reduced FA and increased DR are consistent with reduced organization of the white matter and non-decision time, which is a non-cognitive component of the RT. Thus, the only finding in this sample was response slowing associated with limited, local reduction in white-matter micro-organization. This limited finding suggests that although in healthy adults, non-cognitive

speed may be associated with age-related impairments in diffusion properties of normal WM, such associations are limited to selected locations and selected indices of WM microstructure.

This study has several limitations. First, its cross-sectional design precludes gauging true age-related change, and most notably, individual differences in change (Lindenberger et al., 2011). Indeed, magnitude of the age-related decline in RT had been shown to be underestimated in cross-sectional designs (Schaie, 1989). In addition, cross-sectional designs may lack sensitivity to brain-cognition associations revealed by longitudinal studies (e.g., Raz, Lindenberger, Rodrigue et al., 2005) and have questionable validity in establishing mediators of age-related change (Maxwell & Cole, 2007). Second, all participants in this study were normotensive, healthy adults. Although this sample selection is for the purpose of reducing some confounding factors associated with hypertension and antihypertensive medication, it may conceal the brain-cognition association modified by vascular risk factors. Vascular risk factors may matter more than age for WMH progression and cortical shrinkage in posterior brain regions and accelerated declines in cognitive performance, especially in the domain of executive functions, are associated with elevated vascular risk (Raz, Rodrigue, & Acker, 2003; Raz, Rodrigue, Kennedy, & Acker, 2007). Third, some important pathways such as the uncinate fasciculus and fornix were not included in the analysis because of their particular sensitivity to multiple influences such as head orientation, noise level, image registration and voxel size (Bach et al., 2014). Thus, the role played by the integrity of these white matter tracts in RT parameters remains to be explored. Fourth, the b0 images used for identifying WMH and CSF-filled regions are, in spite of being true T2 images, less than ideal for the task. Use of FLAIR images co-registered with the DTI may be a better alternative. Such approach, however, will involve co-registration step that in its own right may introduce error and bias. Finally, diffusion tensor approach, as implemented in this study and in almost all previous studies, cannot characterize white matter voxels containing crossing fibers and allows no clear neurobiological interpretation of the findings (Jones, Knösche, & Turner, 2013).

In summary, in a sample of healthy adults, we found little evidence of association between diffusion properties of the normal appearing white matter and reaction time parameters. After conservative control for chance findings was applied, only in the body of the corpus callosum was higher DR reliably associated with longer non-decision time. Notably, this limited result was obtained while we replicated all the major findings in the extant literature on RT components and age differences in DTI indices: associations of advanced age with lower drift rate, greater response conservativeness and longer non-decision time as well as smaller FA and larger MD in most examined white matter tracts. Moreover, we confirmed anterior-posterior gradient in age-related decrease in FA and increase in MD, DA, and DR of the corpus callosum and in FA and DR of the internal capsule. Thus, the observed lack of associations between DTI-based indices of normal-appearing white matter and RT components cannot be explained by an atypical sample or measurement methods. Understanding cerebral substrates of age-related cognitive slowing will require longitudinal studies, accounting for vascular risk factors, and employing a wider variety of approaches to gauging brain myelin content (e.g., De Santis et al, 2014).

Acknowledgements

This work was supported by a grant R37 AG011230 from the National Institute on Aging, National Institutes of Health, USA to NR.

References

Bach M, Laun FB, Leemans A, Tax CM, Biessels GJ, Stieltjes B, Maier-Hein KH. Methodological considerations on tract-based spatial statistics (TBSS). Neuroimage. 2014; 100:358–69. doi: 10.1016/j.neuroimage.2014.06.021. Epub 2014 Jun 16. [PubMed: 24945661]

Bagnato F, Hametner S, Yao B, Van Gelderen P, Merkle H, Cantor FK, Duyn JH. Tracking iron in multiple sclerosis: A combined imaging and histopathological study at 7 Tesla. Brain. 2011; 134(12):3599–3612.

Bucur B, Madden DJ, Spaniol J, Provenzale JM, Cabeza R, White LE, Huettel SA. Age-related slowing of memory retrieval: Contributions of perceptual speed and cerebral white matter integrity. Neurobiology of Aging. 2008; 29(7):1070–1079. [PubMed: 17383774]

Burns A, Lawlor B, Craig S. Rating scales in old age psychiatry. British Journal of Psychiatry. 2002; 180(FEB.):161–167. [PubMed: 11823329]

Cerella J. Information processing rates in the elderly. Psychological Bulletin. 1985; 98(1):67–83. [PubMed: 4034819]

Chiang MC, McMahon KL, de Zubicaray GI, Martin NG, Hickie I, Toga AW, Thompson PM. Genetics of white matter development: A DTI study of 705 twins and their siblings aged 12 to 29. NeuroImage. 2011; 54(3):2308–2317. [PubMed: 20950689]

Davis SW, Dennis NA, Buchler NG, White LE, Madden DJ, Cabeza R. Assessing the effects of age on long white matter tracts using diffusion tensor tractography. NeuroImage. 2009; 46(2):530–541. [PubMed: 19385018]

Davis SW, Kragel JE, Madden DJ, Cabeza R. The architecture of cross-hemispheric communication in the aging brain: Linking behavior to functional and structural connectivity. Cerebral Cortex. 2012; 22(1):232–242. [PubMed: 21653286]

Santis S, Drakesmith M, Bells S, Assaf Y, Jones DK. Why diffusion tensor MRI does well only some of the time: variance and covariance of white matter tissue microstructure attributes in the living human brain. Neuroimage. 2014; 89:35–44. doi:10.1016/j.neuroimage.2013.12.003. Epub 2013 Dec 14. [PubMed: 24342225]

Donders FC. On the speed of mental processes. Acta Psychologica. 1868/1969; 30:412–431. [PubMed: 5811531]

Dutilh G, Vandekerckhove J, Forstmann BU, Keuleers E, Brysbaert M, Wagenmakers EJ. Testing theories of post-error slowing. Attention, Perception, and Psychophysics. 2012; 74(2):454–465.

Felmingham KL, Baguley IJ, Green AM. Effects of diffuse axonal injury on speed of information processing following severe traumatic brain injury. Neuropsychology. 2004; 18(3):564–571. [PubMed: 15291734]

Folstein MF, Folstein SE, McHugh PR. “Mini-mental state”. A practical method for grading the cognitive state of patients for the clinician. Journal of Psychiatry Research. 1975; 12:189–198.

Gunning-Dixon FM, Raz N. The cognitive correlates of white matter abnormalities in normal aging: A quantitative review. Neuropsychology. 2000; 14(2):224–232. [PubMed: 10791862]

Head D, Buckner RL, Shimony JS, Williams LE, Akbudak E, Conturo TE, Snyder AZ. Differential Vulnerability of Anterior White Matter in Nondemented Aging with Minimal Acceleration in Dementia of the Alzheimer Type: Evidence from Diffusion Tensor Imaging. Cerebral Cortex. 2004; 14(4):410–423. [PubMed: 15028645]

Hu LT, Bentler PM. Cutoff criteria for fit indexes in covariance structure analysis: Conventional criteria versus new alternatives. Structural Equation Modeling. 1999; 6(1):1–55.

ICO. Visual Acuity Measurement Standard. 1984

Inano S, Takao H, Hayashi N, Abe O, Ohtomo K. Effects of age and gender on white matter integrity. American Journal of Neuroradiology. 2011; 32(11):2103–2109. [PubMed: 21998104]

Jones DK, Knösche TR, Turner R. White matter integrity, fiber count, and other fallacies: The do's and don'ts of diffusion MRI. NeuroImage. 2013; 73:239–254. [PubMed: 22846632]

Kennedy KM, Raz N. Pattern of normal age-related regional differences in white matter microstructure is modified by vascular risk. Brain Research. 2009; 1297:41–56. [PubMed: 19712671]

Kerchner GA, Racine CA, Hale S, Wilheim R, Laluz V, Miller BL, Kramer JH. Cognitive processing speed in older adults: Relationship with white matter integrity. PLoS ONE. 2012; 7(11)

Lindenberger U, von Oertzen T, Ghisletta P, Hertzog C. Cross-sectional age variance extraction: What's change got to do with it? Psychology and Aging. 2011; 26(1):34–47. doi:10.1037/a0020525. [PubMed: 21417539]

Liston C, Watts R, Tottenham N, Davidson MC, Niogi S, Ulug AM, Casey BJ. Frontostriatal microstructure modulates efficient recruitment of cognitive control. Cerebral Cortex. 2006; 16(4):553–560. [PubMed: 16033925]

Madden DJ, Bennett IJ, Song AW. Cerebral white matter integrity and cognitive aging: Contributions from diffusion tensor imaging. Neuropsychology Review. 2009a; 19(4):415–435. [PubMed: 19705281]

Madden DJ, Spaniol J, Costello MC, Bucur B, White LE, Cabeza R, Huettel SA. Cerebral white matter integrity mediates adult age differences in cognitive performance. Journal of Cognitive Neuroscience. 2009b; 21(2):289–302. [PubMed: 18564054]

Maillard P, Carmichael O, Harvey D, Fletcher E, Reed B, Mungas D, DeCarli C. FLAIR and diffusion MRI signals are independent predictors of white matter hyperintensities. AJNR Am J Neuroradiol. 2013; 34(1):54–61. doi:10.3174/ajnr.A3146. [PubMed: 22700749]

Matzke D, Wagenmakers EJ. Psychological interpretation of the ex-gaussian and shifted wald parameters: A diffusion model analysis. Psychonomic Bulletin and Review. 2009; 16(5):798–817. [PubMed: 19815782]

Maxwell SE, Cole DA. Bias in cross-sectional analyses of longitudinal mediation. Psychological Methods. 2007; 12(1):23–44. [PubMed: 17402810]

Mori, S.; Wakana, S.; Nagae-Poetscher, LM.; van Zijl, PCM. MRI Atlas of Human White Matter. The Netherlands Elsevier; Amsterdam: 2005.

Muthén, L.; Muthén, B. Mplus User's Guide. 7th ed.. Muthén & Muthén; Los Angeles: 2012.

O'Connor DW, Pollitt PA, Hyde JB, Fellows JL, Miller ND, Brook CPB, Reiss BB. The reliability and validity of the Mini-Mental State in a British community survey. Journal of Psychiatric Research. 1989; 23(1):87–96. [PubMed: 2666647]

Oldfield RC. The assessment and analysis of handedness: the Edinburgh inventory. Neuropsychologia. 1971; 9:97–113. [PubMed: 5146491]

Pal D, Trivedi R, Saksena S, Yadav A, Kumar M, Pandey CM, Gupta RK. Quantification of age- and gender-related changes in diffusion tensor imaging indices in deep grey matter of the normal human brain. Journal of Clinical Neuroscience. 2011; 18(2):193–196. [PubMed: 21183352]

Paling D, Tozer D, Wheeler-Kingshott C, Kapoor R, Miller DH, Golay X. Reduced R2' in multiple sclerosis normal appearing white matter and lesions may reflect decreased myelin and iron content. Journal of Neurology, Neurosurgery and Psychiatry. 2012; 83(8):785–792. doi:10.1136/jnnp-2012-302541.

Radloff LS. The CES-D scale: a self-report depression scale for research in the general population. Applied Psychological Measurement. 1977; 1:385–401.

Ratcliff R. A theory of memory retrieval. Psychological Review. 1978; 85:59–108.

Ratcliff R. The EZ diffusion method: Too EZ? Psychonomic Bulletin and Review. 2008a; 15(6):1218–1228. [PubMed: 19001593]

Ratcliff R. Modeling Aging Effects on Two-Choice Tasks: Response Signal and Response Time Data. Psychology and Aging. 2008b; 23(4):900–916. [PubMed: 19140659]

Ratcliff R, McKoon G. The diffusion decision model: Theory and data for two-choice decision tasks. Neural Computation. 2008; 20(4):873–922. [PubMed: 18085991]

Ratcliff R, Thapar A, McKoon G. The effects of aging on reaction time in a signal detection task. Psychology and Aging. 2001; 16(2):323–341. [PubMed: 11405319]

Ratcliff R, Thapar A, McKoon G. Aging and individual differences in rapid two-choice decisions. Psychonomic Bulletin and Review. 2006; 13(4):626–635. [PubMed: 17201362]

Ratcliff R, Thapar A, McKoon G. Application of the diffusion model to two-choice tasks for adults 75-90 years old. Psychology and Aging. 2007; 22(1):56–66. [PubMed: 17385983]

Raz N, Rodrigue KM, Acker JD. Hypertension and the Brain: Vulnerability of the Prefrontal Regions and Executive Functions. Behavioral Neuroscience. 2003; 117(6):1169–1180. [PubMed: 14674838]

Raz N, Lindenberger U, Rodrigue KM, Kennedy KM, Head D, Williamson A, Dahle C, Gerstorf D, Acker JD. Regional brain changes in aging healthy adults: General trends, individual differences, and modifiers. Cerebral Cortex. 2005; 15:1676–1689. [PubMed: 15703252]

Raz N, Rodrigue KM, Kennedy KM, Acker JD. Vascular health and longitudinal changes in brain and cognition in middle-aged and older adults. Neuropsychology. 2007; 21(2):149–157. [PubMed: 17402815]

Salthouse TA. Adult age and the speed-accuracy trade-off. Ergonomics. 1979; 22(7):811–821. [PubMed: 488072]

Salthouse TA. Converging evidence for information-processing stages: A comparative-influence stage-analysis method. Acta Psychologica. 1981; 47(1):39–61.

Salthouse, TA. Theoretical perspectives on cognitive aging. Lawrence Erlbaum Associates; Hillsdale, New Jersey: 1991.

Sasson E, Doniger GM, Pasternak O, Assaf Y. Structural correlates of memory performance with diffusion tensor imaging. NeuroImage. 2010; 50(3):1231–1242. [PubMed: 20045476]

Sasson E, Doniger GM, Pasternak O, Tarrasch R, Assaf Y. Structural correlates of cognitive domains in normal aging with diffusion tensor imaging. Brain Structure and Function. 2012; 217(2):503–515. [PubMed: 21909706]

Saunders B, Jentzsch I. False external feedback modulates posterror slowing and the f-P300: Implications for theories of posterror adjustment. Psychonomic Bulletin and Review. 2012; 19(6): 1210–1216. [PubMed: 22987148]

Schaie KW. Perceptual speed in adulthood: Cross-sectional and longitudinal studies. Psychology and Aging. 1989; 4(4):443–453. doi:10.1037/0882-7974.4.4.443. [PubMed: 2619951]

Smith SM, Jenkinson M, Johansen-Berg H, Rueckert D, Nichols TE, Mackay CE, Behrens TEJ. Tract-based spatial statistics: Voxelwise analysis of multi-subject diffusion data. NeuroImage. 2006; 31(4):1487–1505. [PubMed: 16624579]

Smith SM. Fast robust automated brain extraction. Human Brain Mapping. 2002; 17(3):143–155. [PubMed: 12391568]

Sternberg S. Memory-scanning: mental processes revealed by reaction-time experiments. American Scientist. 1969; 57(4):421–457. [PubMed: 5360276]

Sullivan EV, Adalsteinsson E, Hedehus M, Ju C, Moseley M, Lim KO, Pfefferbaum A. Equivalent disruption of regional white matter microstructure in ageing healthy men and women. NeuroReport. 2001; 12(1):99–104. [PubMed: 11201100]

Sullivan EV, Pfefferbaum A. Diffusion tensor imaging and aging. Neuroscience and Biobehavioral Reviews. 2006; 30(6):749–761. [PubMed: 16887187]

Sullivan EV, Rohlfing T, Pfefferbaum A. Longitudinal study of callosal microstructure in the normal adult aging brain using quantitative DTI fiber tracking. Developmental Neuropsychology. 2010; 35(3):233–256. [PubMed: 20446131]

Thapar A, Ratcliff R, McKoon G. A diffusion model analysis of the effects of aging on letter discrimination. Psychology and Aging. 2003; 18(3):415–429. [PubMed: 14518805]

Turken A, Whitfield-Gabrieli S, Bammer R, Baldo JV, Dronkers NF, Gabrieli JDE. Cognitive processing speed and the structure of white matter pathways: Convergent evidence from normal variation and lesion studies. NeuroImage. 2008; 42(2):1032–1044. [PubMed: 18602840]

Vandekerckhove J, Tuerlinckx F. Diffusion model analysis with MATLAB: A DMAT primer. Behavior Research Methods. 2008; 40(1):61–72. doi:10.3758/brm.40.1.61. [PubMed: 18411528]

Vernooij MW, de Groot M, van der Lugt A, Ikram MA, Krestin GP, Hofman A, Breteler MMB. White matter atrophy and lesion formation explain the loss of structural integrity of white matter in aging. NeuroImage. 2008; 43(3):470–477. [PubMed: 18755279]

Voss A, Rothermund K, Voss J. Interpreting the parameters of the diffusion model: Anempirical validation. Memory and Cognition. 2004; 32(7):1206–1220. [PubMed: 15813501]

WHO. Grades of hearing impairment. Hearing Network News. 1991

Wheeler-Kingshott CAM, Cercignani M. About “axial” and “radial” diffusivities. Magnetic Resonance in Medicine. 2009; 61(5):1255–1260. [PubMed: 19253405]

Zhang Y, Brady M, Smith S. Segmentation of brain MR images through a hidden Markov random field model and the expectation-maximization algorithm. IEEE Trans Med Imag. 2001; 20(1):45–57.

HIGHLIGHTS

- We examined associations of white matter and reaction time components in healthy adults.
- White matter hyperintensities that could affect DTI parameters was excluded.
- We replicated age differences in RT and WM and extended them to adult lifespan.
- However, DTI indices of normal WM integrity were largely unrelated to RT components.

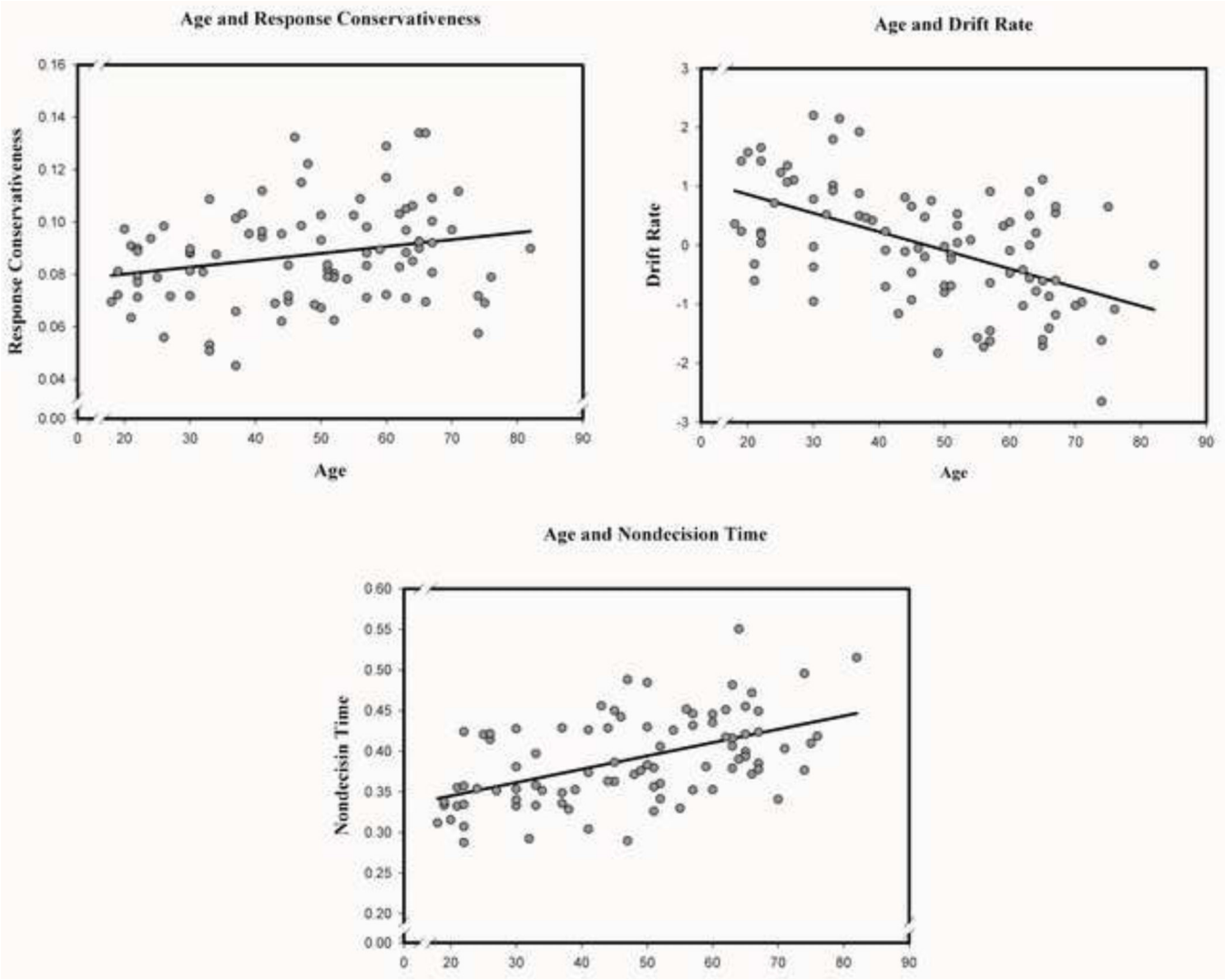

Figure 1.

Association between age and RT components according to the Diffusion Model (Ratcliff, 1978): Drift rate, Response conservativeness, and Non-decision time.

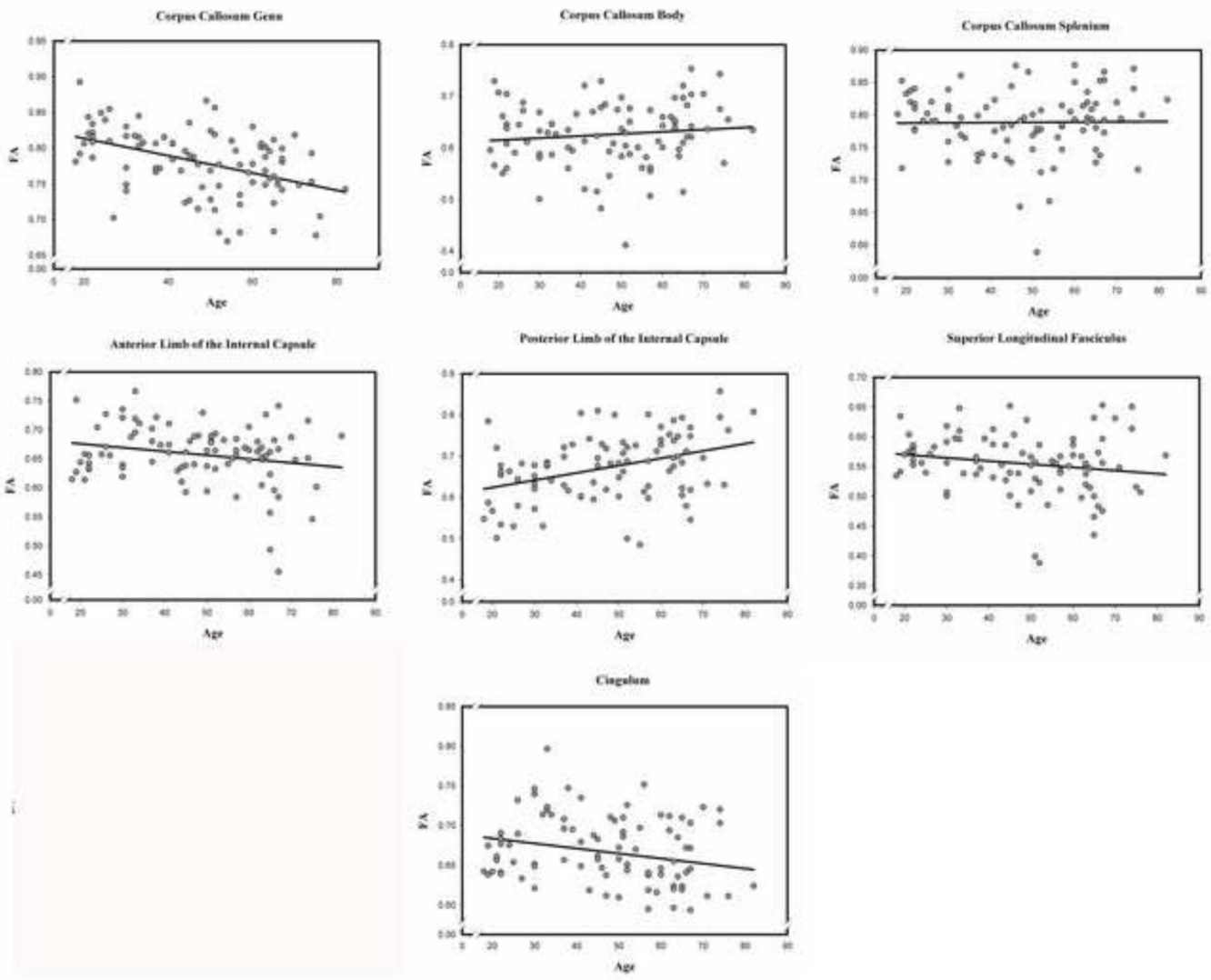

Figure 2.

Associations between age and fractional anisotropy (FA) in each of the examined normal appearing white matter regions.

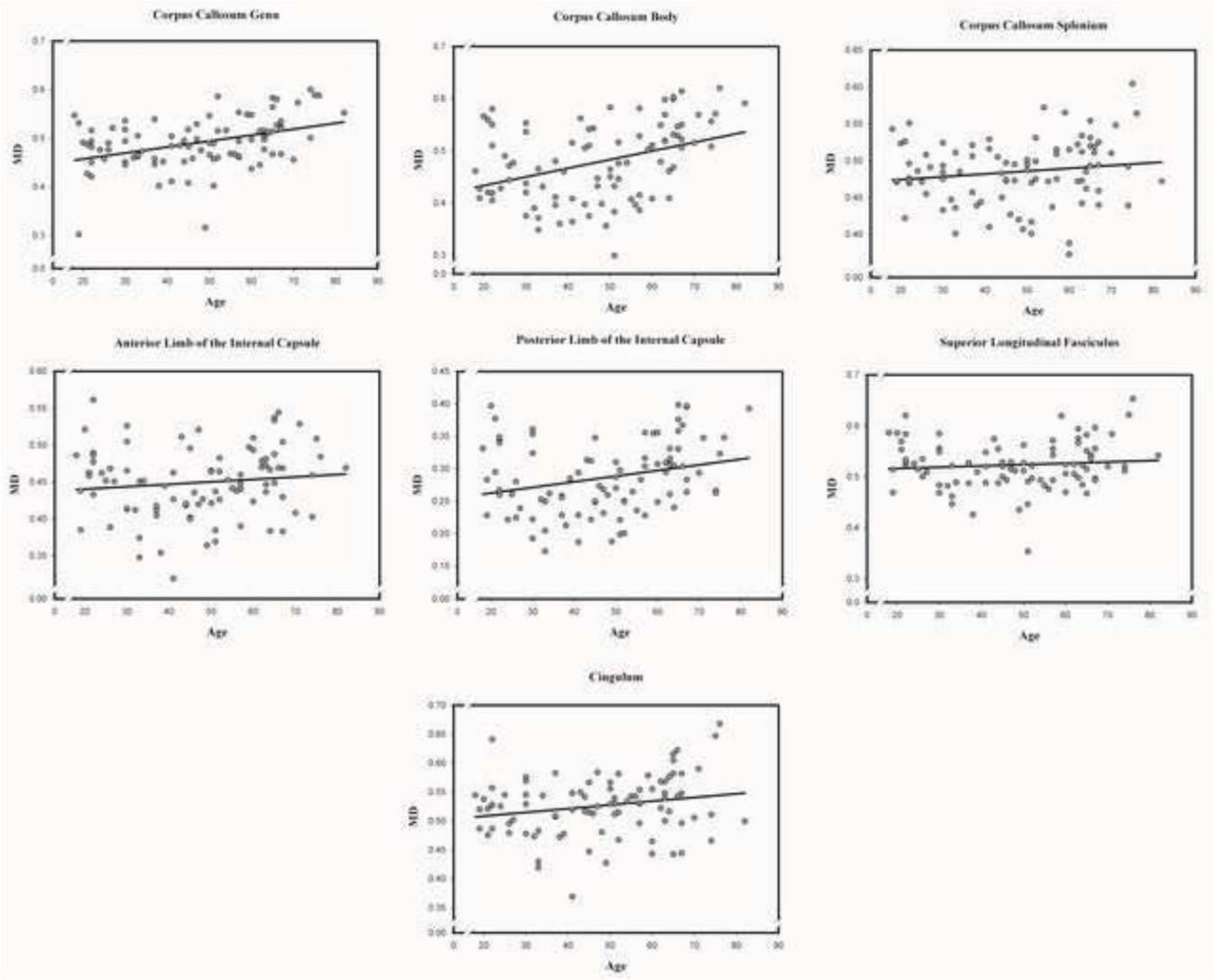

Figure 3.

Association between age and mean diffusivity (MD) in each of the examined normal appearing white matter regions.

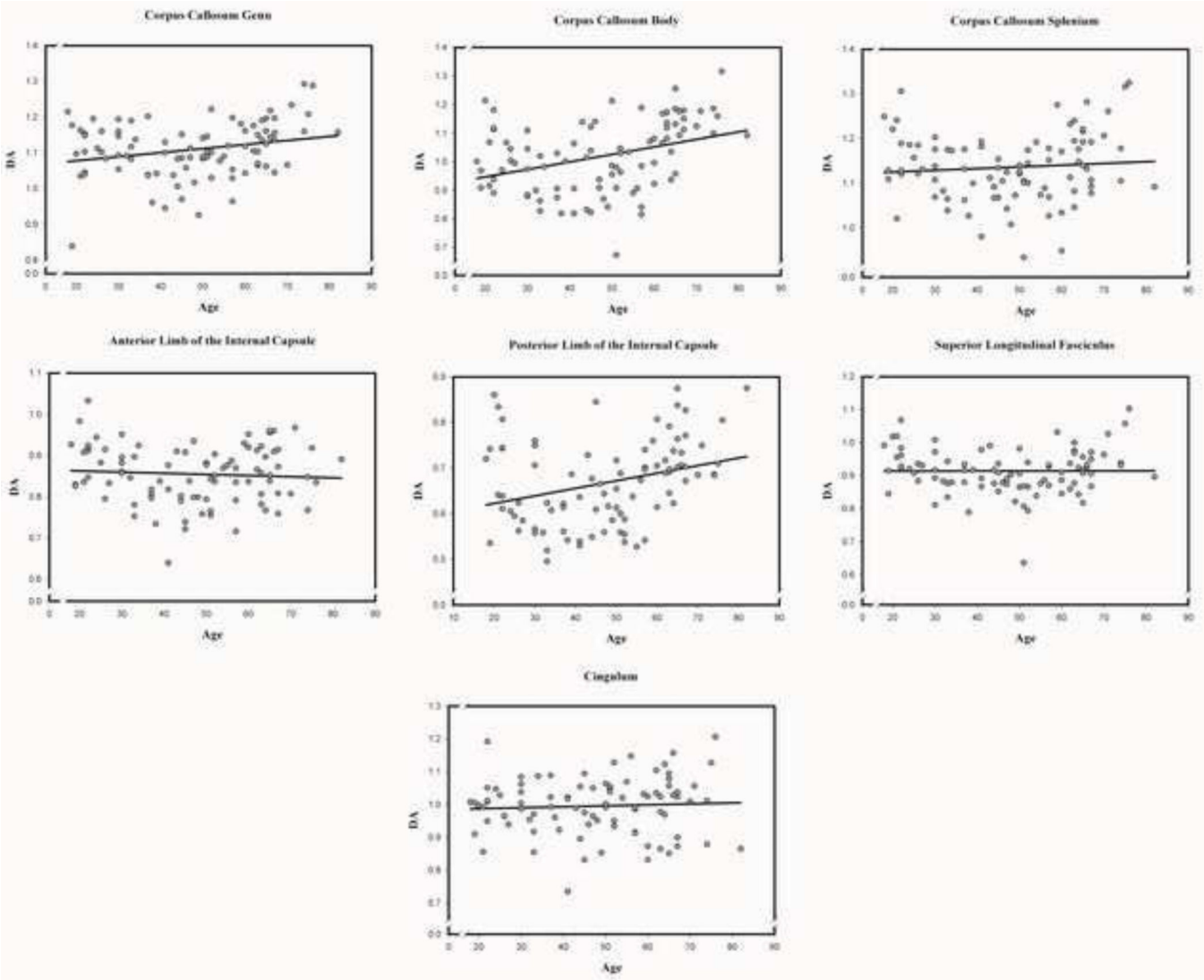

Figure 4.

Association between age and axial diffusivity (DA) in each of the examined normal appearing white matter regions.

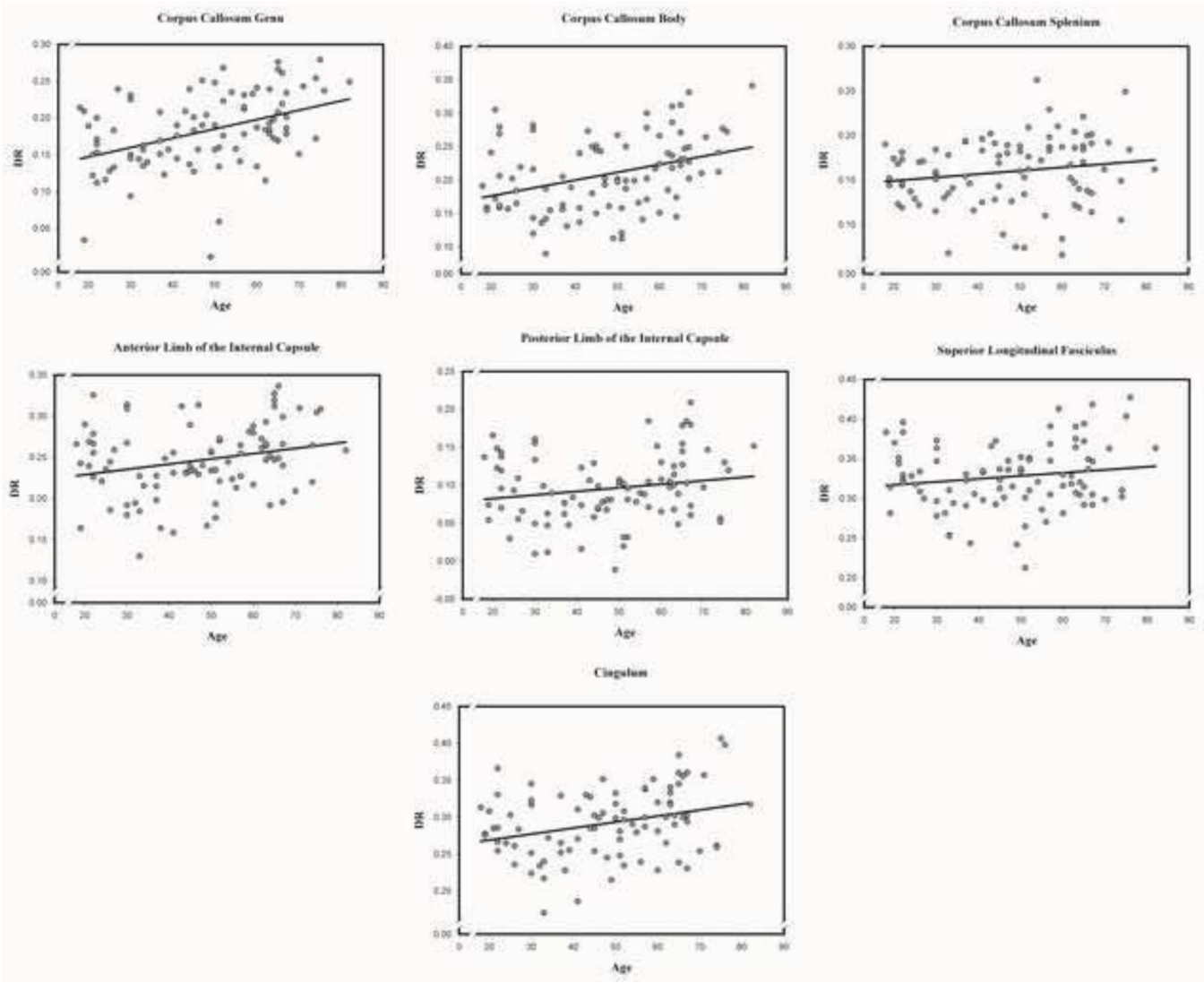

Figure 5.

Association between age and radial diffusivity (DR) in each of the examined normal appearing white matter regions.

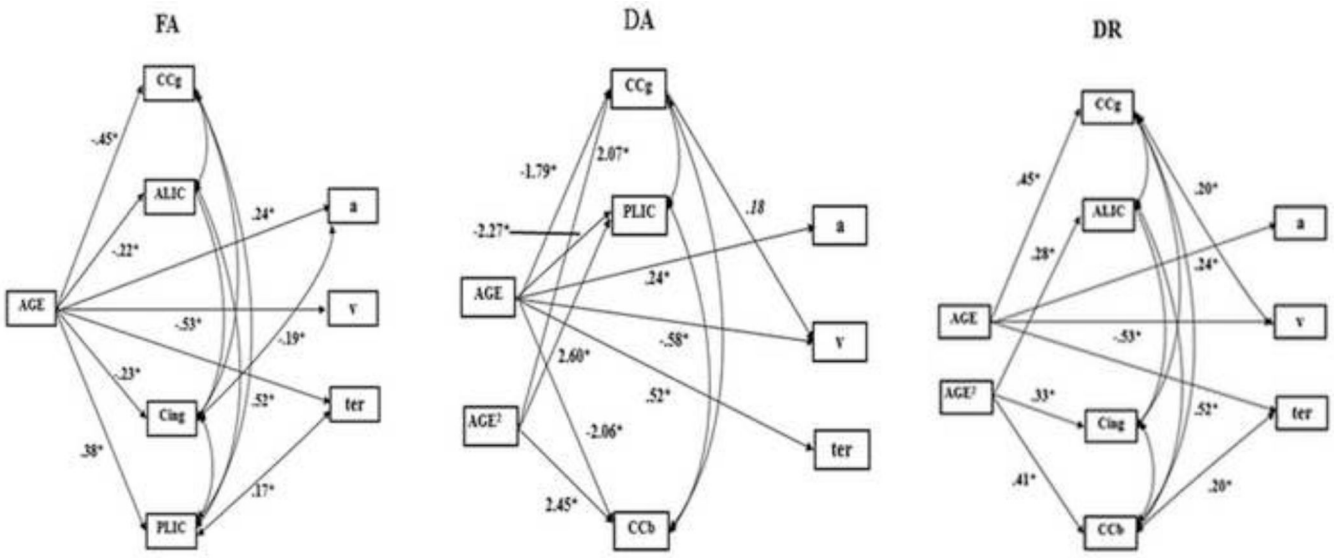

Figure 6.

Path models for the associations between regional DTI indices, FA, DA, and DR in normal-appearing white matter, and three RT components: drift rate (v), response conservativeness (a) and non-decision time (ter). Abbreviated labels of the white matter regions: CCg: the genu of the corpus callosum; ALIC: the anterior limb of the internal capsule; Cing: the cingulum; PLIC: the posterior limb of the internal capsule; CCb: the body of the corpus callosum.

Table 1

Sample descriptors: A statistical summary.

	Total	Women	Men	*t*	*p*
N	90	60	30		
Age (years)	47.39±16.87	47.6±16.41	46.97±18.04	0.16	0.87
Education (years)	15.28±2.05	15.22±2.28	15.4±1.52	−0.45	0.65
MMSE	28.69±1.07	28.8±0.99	28.47±1.20	1.32	0.19
Systolic BP (mm Hg)	120.74±13.91	120.02±13.34	122.19±15.13	−0.67	0.51
Diastolic BP (mm Hg)	76.08±8.08	75.14±7.08	77.96±9.63	−1.43	0.16

Table 2

Descriptive statistics for accuracy and reaction time measures across task conditions.

	Accuracy				Reaction time			
Condition	**Mean**	**SD**	**CV**	r_{age}	**Mean**	**SD**	**CV**	r_{age}
D 13	0.67	0.10	0.14	−.59	526.28	81.05	0.15	0.65
D 26	0.78	0.12	0.15	−.55	505.77	77.41	0.15	0.62
D 39	0.88	0.08	0.10	−.53	479.33	69.59	0.15	0.65
D 52	0.92	0.07	0.08	−.53	465.00	66.26	0.14	0.64
D 66	0.94	0.06	0.06	−.47	456.62	64.67	0.14	0.62
D 80	0.94	0.06	0.06	−.41	461.95	63.57	0.14	0.63
Mean	0.85	0.07	0.09	−.57	479.02	67.58	0.14	0.65

Note. D: duration of stimulus presentation; CV: coefficient of variation; rage: correlation between age and a model parameter mean; all significant at $p < .05$.

Table 3

Descriptive statistics for three RT components.

	Drift Rate			Response Conservativeness			Non-decision time		
Condition	**Mean**	**SD**	**CV**	**Mean**	**SD**	**CV**	**Mean**	**SD**	**CV**
D 13	0.17	0.11	0.66						
D 26	0.34	0.19	0.56						
D 39	0.60	0.30	0.51						
D 52	0.83	0.44	0.54	0.087	0.019	0.21	0.39	0.054	0.14
D 66	1.01	0.64	0.63						
D 80	0.99	0.65	0.66						

Note. D: duration of stimulus presentation; CV: coefficient of variation.

Table 4

Correlations between age and DTI indices across white matter tracts.

ROI	r_{age_FA}	r_{age_MD}	r_{age_DA}	r_{age_DR}
CCg	-0.44^{***}	0.41^{***}	0.25^{*}	0.43^{***}
CCb	0.11	0.38^{***}	0.36^{**}	0.36^{**}
CCs	0.02	0.15	0.09	0.17
ALIC	-0.21^{*}	0.12	−0.07	0.25^{*}
PLIC	0.38^{***}	0.26^{*}	0.30^{**}	0.18
SLF	−0.19	0.09	0.01	0.16
Cing	-0.24^{*}	0.21^{*}	0.06	0.30^{**}

Note. CCg: the genu of the corpus callosum; CCb: the body of the corpus callosum; CCs: the splenium of the corpus callosum; ALIC: the anterior limb of the internal capsule; PLIC: the posterior limb of the internal capsule; SLF: the superior longitudinal fasciculus; Cing: the cingulum.

* $p < 0.05$

** $p < 0.01$

*** $p < 0.001$.

Table 5

GLM results of age difference in DTI indices in normal-appearing white matter.

ROI	FA		MD		DA		DR	
	***F* (df)**	**P**	***F* (df)**	**P**	***F* (df)**	**P**	**F(df)**	**P**
CCg	23.76 (1, 86)	***	18.27(1, 86)	***	5.48 (1, 86)	*	20.77 (1, 86)	***
CCb	1.24 (1, 86)	ns	18.82 (1, 86)	***	15.84 (1, 86)	***	16.78 (1, 86)	***
CCs	0.14 (1, 86)	ns	2.56 (1, 86)	ns	1.02 (1, 86)	ns	2.85 (1, 86)	ns
ALIC	5.30 (1, 86)	*	1.72 (1, 86)	ns	0.39 (1, 86)	ns	7.76 (1, 86)	**
PLIC	16.12 (1, 86)	***	8.30 (1, 86)	**	12.33 (1, 86)	**	3.48 (1, 86)	ns
SLF	3.23 (1, 86)	ns	2.52 (1, 86)	ns	0.51 (1, 86)	ns	4.92 (1, 86)	*
Cing	7.05 (1, 86)	* *	6.83 (1, 86)	*	0.81 (1, 86)	ns	13.09 (1, 86)	***

Note. CCg: the genu of the corpus callosum; CCb: the body of the corpus callosum; CCs: the splenium of the corpus callosum; ALIC: the anterior limb of the internal capsule; PLIC: the posterior limb of the internal capsule; SLF: the superior longitudinal fasciculus; Cing: the cingulum.

* $p < 0.05$

** $p < 0.01$

*** $p < 0.001$.

Table 6

Comparison of correlations between age with DA and DR across white matter tracts in normal-appearing and whole white matter.

	ROI	r_{ageN}	r_{ageW}	Steiger's Z	p
FA	CCg	**−0.44**	**−0.45**	.23	ns
	CCb	0.11	**−0.31**	3.04	<.01
	CCs	0.02	−0.17	2.01	<.05
	AIC	**−0.21**	**−0.33**	2.48	<.05
	PIC	**0.38**	−0.06	4.90	<.01
	SLF	−0.19	**−0.21**	.33	ns
	Cing	**−0.24**	**−0.28**	1.93	ns
MD	CCg	**0.41**	**0.47**	−1.28	ns
	CCb	**0.38**	**0.33**	.46	ns
	CCs	0.15	0.04	1.31	ns
	AIC	0.12	0.12	0	ns
	PIC	**0.26**	−0.18	4.37	<.01
	SLF	0.09	**0.24**	−1.42	ns
	Cing	**0.21**	0.20	.39	ns
DA	CCg	**0.25**	**0.33**	−1.53	ns
	CCb	**0.36**	0.15	1.54	ns
	CCs	0.09	−0.02	1.15	ns
	AIC	−0.07	−0.03	−.53	ns
	PIC	**0.30**	**−0.27**	**4.50**	<.01
	SLF	0.01	0.16	−1.24	ns
	Cing	0.06	0.05	.47	ns
DR	CCg	**0.43**	**0.49**	−2.0	<.05
	CCb	**0.36**	**0.36**	0	ns
	CCs	0.17	0.10	1.41	ns
	AIC	**0.25**	**0.25**	0	ns
	PIC	0.18	−0.07	4.00	<.01
	SLF	0.16	**0.26**	−1.24	ns
	Cing	**0.30**	**0.29**	.49	ns

Note. CCg: the genu of the corpus callosum; CCb: the body of the corpus callosum; CCs: the splenium of the corpus callosum; ALIC: the anterior limb of the internal capsule; PLIC: the posterior limb of the internal capsule; SLF: the superior longitudinal fasciculus; Cing: cingulum; Significant linear age correlations are bolded; r_{ageN}: association with age in normal-appearing white matter; r_{ageW} :association with age in whole white matter.

Table 7

Goodness-of-fit indices for path models.

	Models	χ^2	df	χ^2/df	p	CFI	TLI	RMSEA
FA	**The final model**	20.83	21	0.99	.47	1.00	1.00	.00
	The final model	13.53	15	0.90	.56	1.00	1.01	.00
DA	**The reversed model**	14.09	15	0.94	.52	1.00	1.01	.00
	The correlational model	14.09	15	0.94	.52	1.00	1.01	.00
	The final model	20.23	20	1.01	.44	1.00	1.00	.01
	The v reversed model	19.87	20	0.99	.47	1.00	1.00	.00
DR	**The ter reversed model**	17.94	20	0.90	.59	1.00	1.01	.00
	The correlational model	16.47	20	0.82	.69	1.00	1.02	.00

Notes: CFI: Comparative Fit Index; TLI: Tucker–Lewis Index; and RMSEA: Root mean square error of approximation; v: drift rate; ter: non-decision time.